

# HOTSPOT VALIDATION OF THE HIMAWARI-8 SATELLITE BASED ON MULTISOURCE DATA FOR CENTRAL KALIMANTAN

Khalifah Insan Nur Rahmi<sup>1\*</sup>, Sayidah Sulma, Indah Prasasti

<sup>1</sup>Remote Sensing Applications Centre, LAPAN

Jl. Kalisari No. 8, Pekayon, Pasar Rebo, Jakarta Timur, Indonesia

\*e-mail: [khalifah.insan@lapan.go.id](mailto:khalifah.insan@lapan.go.id)

Received:17 January 2020; Revised: 17 February 2020; Approved: 18 February 2020

**Abstract** The Advanced Himawari Imager (AHI) is the sensor aboard the remote-sensing satellite Himawari-8 which records the Earth's weather and land conditions every 10 minutes from a geostationary orbit. The imagery produced known as Himawari-8 has 16 bands which cover visible, near infrared, middle infrared and thermal infrared wavelength potentials to monitor forestry phenomena. One of these is forest/land fires, which frequently occur in Indonesia in the dry season. Himawari-8 can detect hotspots in thermal bands 5 and band 7 using absolute fire pixel (AFP) and possible fire pixel (PFP) algorithms. However, validation has not yet been conducted to assess the accuracy of this information. This study aims to validate hotspots identified from Himawari images based on information from Landsat 8 images, field surveys and burnout data. The methodology used to validate hotspots comprises AFP and PFP extraction, determining firespots from Landsat 8, buffering at 2 km from firespots, field surveys, burnout data, and calculation of accuracy. AFP and PFP hotspot validation of firespots from Landsat-8 is found to have higher accuracy than the other options. In using Himawari-8 hotspots to detect land/forest fires in Central Kalimantan, the AFP algorithm with 2km radius has accuracy of 51.33% while the PFP algorithm has accuracy of 27.62%.

Keywords: *hotspot, Himawari-8, validation, Landsat-8, forest/land fire*

## 1 INTRODUCTION

The Advanced Himawari Imager is an optical remote-satellite sensor which records the Earth's weather and land conditions. It is located on a geostationary satellite which records images every 10 minutes (Kushardono, 2012). The imagery is known as Himawari-8 and consists of 16 bands, one being a thermal band which can identify land surface temperature (LST) (Choi & Suh, 2018). One use of LST is to identify hotspots related to forest/land fires (Choi & Suh, 2018; Vlassova et al., 2014; Guangmeng & Mei, 2004). Himawari-8 also has a reflectant band that records objects based on their reflectant value. This data is distributed through the Himawari cast as two data types, Himawari Standard Data (HSD)

and NetCDF L1 gridded data with 2.2 km spatial resolution (JMA, 2017).

Forest/land fires often occur in Indonesia, particularly in Kalimantan, Sumatra and Papua. Fires which occur in peatland areas (Puspa, Sukaesih, & Syaufina, 2016; Hayasaka, Noguchi, Putra, Yulianti, & Vadrevu, 2014; Osaki, Nursyamsi, Noor, Wahyunto, & Segah 2016) emit thick smoke and last longer than other types of fire (Noor, 2019). Such fires impact on environmental conditions and contribute to air pollution. To aid prevention, remote-sensing technology is used to monitor forest/land fires based on hotspot distribution. MODIS imagery using Terra or Aqua satellites has been used to successfully monitor hotspots (Giglio, Schroeder, & Justice, 2016;

Giglio, Csiszar, & Justice, 2006; LAPAN, 2016; Tanpipat, Kiyoshi, & Prayoonpong, 2009) such as by FIRMS-NASA, with accuracy of 64%, and Indofire, with accuracy of 42% (Zubaidah Vetrita, & Rokhis Khomarudin, 2014). MODIS hotspot information recorded twice a day is available on the LAPAN system (at <http://modis-catalog.lapan.go.id/monitoring/>) with confidence levels of low (0–30%), medium (30–60%), and high (60–100%) (LAPAN, 2016).

Since the release of Himawari-8, several studies of forest/land fires have been conducted, including Fitriana et al. (2018), Hally, Wallace, Reinke, and Jones (2016) and Suwarsono et al., (n.d.). Initially, identification of forest fire was based on visual interpretation of smoke haze using RGB combinations from bands 3, 4, and 6 of AHI8 (Pandjaitan & Panjaitan, 2015). Then, hotspot pixels at 500 m resolution using multi-spatial resolution of band 7 (2 km), band 4 (1 km), and band 3 (500 m) were used (Suwarsono et al., n.d.). In Australia, 500 m resolution thermal band identification of hotspots using an FSA algorithm has yielded 80% accuracy (Hally et al., 2016).

The objective of this study is to validate hotspots in Himawari-8 imagery. Study of Himawari-8 hotspots has been conducted by Suwarsono et al. (n.d.), and used two algorithms to derive hotspots – absolute fire pixel (AFP) and possible fire pixel (PFP). This study aims to check the accuracy of hotspots in Central Kalimantan derived from these algorithms using Landsat 8 images, field survey data and burnout data. Validated hotspots could be used to complement

other hotspot data. Ten-minute hotspot data could be used for real-time monitoring of forest/land fires to provide alerts to prevent further losses.

## **2 MATERIALS AND METHODOLOGY**

### **2.1 Location and data**

The data used in this study are AFP- and PFP-derived Himawari-8 hotspot data, composite RGB 654 Landsat 8 images, field survey data and burnout data. The AFP and PFP hotspot data used are taken from the period 1 September 2018 to 10 October 2018, the survey data is from 27 September to 6 October 2018, and the burnout data is from BPBD Kab. Kapuas (the regional disaster management agency) from 1 September 2018 to 7 October 2018. Table 2.1. lists the data used in this study.

Himawari-8 data is obtained from the FTP JAXA P-tree system download. The Himawari-8 data is already in the form of a data grid in which all bands have been processed geometrically and radiometrically with 2.2 km spatial resolution for 16 bands. The 16 bands have spectral range from 0.46 to 13.3  $\mu\text{m}$ , consisting of three visible bands (0.46–0.64  $\mu\text{m}$ ), three near infrared bands (0.86–2.3  $\mu\text{m}$ ) and ten thermal infrared bands (3.9–13.3  $\mu\text{m}$ ) (JMA, 2017). Because of their availability, thermal and reflectant bands were chosen in this study to detect hotspots. In addition, the short revisit time of 10 minutes makes this data appropriate for monitoring dynamic earth-surface phenomena, one of which is LST used for hotspot identification. The specifications of the Himawari-8 imagery are shown in Table 2.2

Table 2.1: List of data used in this study

No	Data	Date
1.	AFP and PFP Himawari 8 hotspot data	01 Sept – 10 Oct 2018
2.	Composite RGB 654 Landsat 8 data	28 Sept 2018
3.	Field survey data	27 Sept – 6 Oct 2018
4.	Burnout data	03 Sept – 07 Oct 2018

Table 2.2: Image characteristics of Himawari 8

Band	Central wavelength ( $\mu\text{m}$ )	Spectral group	Spatial resolution (m)	Gridded data spatial resolution (m)
1	0.46	Visible	1000	2200
2	0.51	Visible	1000	2200
3	0.64	Visible	500	2200
4	0.86	NIR	1000	2200
5	1.6	NIR	2000	2200
6	2.3	NIR	2000	2200
7	3.9	Thermal IR	2000	2200
8	6.2	Thermal IR	2000	2200
9	7.0	Thermal IR	2000	2200
10	7.3	Thermal IR	2000	2200
11	8.6	Thermal IR	2000	2200
12	9.6	Thermal IR	2000	2200
13	10.4	Thermal IR	2000	2200
14	11.2	Thermal IR	2000	2200
15	12.3	Thermal IR	2000	2200
16	13.3	Thermal IR	2000	2200

Landsat 8 RGB 654 composite is an image combination which can be used to see the visual appearance of objects in burned areas (LAPAN, 2015). Landsat 8 image data with L1TP correction level, in which the data has been radiometrically and geodetically corrected based on GCP and DEM (USGS, 2019), was obtained from LAPAN. In this study, we used 30 m

Landsat 8 of the study area is located on path/row 118/062, as shown in Figure 2.1. The area covers three regencies/cities of Central Kalimantan Province, including Palangkaraya City, Pulang Pisau Regency and Kapuas

resolution Landsat 8 imagery as validation data. Additional data is composite images of Himawari-8 RGB natural colour 346. This composite provides a general appearance of the study area to distinguish land, ocean, cloud and fire/smoke objects. Based on Pandjaitan and Panjaitan (2015), fire and smoke appears as brownish yellow objects in the band combinations. Regency. Most of the study sites are peatlands, but there is also a small portion in the form of mineral soil. On peatlands, land cover may be in the form of vegetation including oil palms or shrubs.

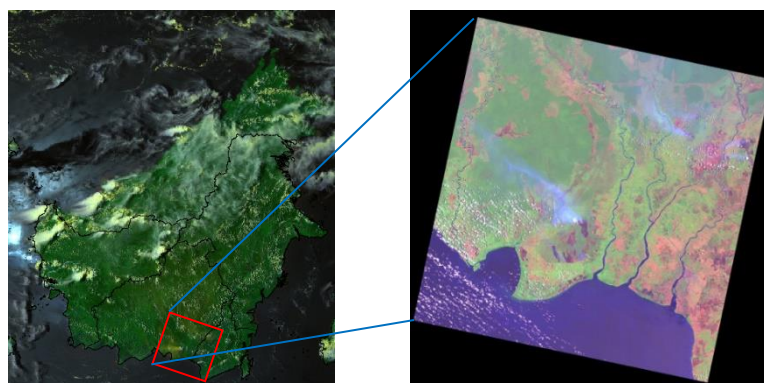


Figure 2.1: RGB composite of Himawari-8 and Landsat 8 images of the study area

## 2.3 Methods

A Himawari-8 hotspot is the centre point of a hotspot pixel, while the hotspot itself is a pixel extracted from remote-sensing images that have a higher temperature than their surroundings based on temperature thresholds. A hotspot is usually used as a forest/land fire indicator in which the more hotspots there are the higher the forest/land fire potency (LAPAN, 2016). The Himawari-8 image has been corrected and has coordinates matching the field locations. The range of reflectant values is from 0–1 in the optical band and in hundreds of kelvin units in the thermal band. The method used in this study consists of extracting AFP and PFP hotspots, cloud masking, water masking, sunglint masking, determination of firespots, buffering at 2 km from firespots, and validation.

### a. Extraction of AFP and PFP hotspots

Based on Suwarsono et al., (n.d.), the AFP hotspot algorithm is extracted from a thermal infrared band (3.9  $\mu\text{m}$ ) that is sensitive to hotspots (JMA, 2017) as shown in formula 1:

$$\text{AFP} = T_{3.9} \geq 320 \text{ K} \quad (2-1)$$

PFP hotspots (Suwarsono et al., (n.d.)) are also derived from the 3.9  $\mu\text{m}$  thermal infrared band and the difference between the 3.9  $\mu\text{m}$  band and the 11.2  $\mu\text{m}$  band. This algorithm is an adaptation from the MODIS hotspot algorithm (MOD14). Band 11.2  $\mu\text{m}$  is a thermal infrared band that is sensitive to small fires or hotspots based on surface temperature.

$$\text{PFP} = T_{3.9} \geq 310 \text{ K and } T_{3.9} - T_{11.2} \geq 12.5 \text{ K} \quad (2-2)$$

### b. Cloud masking

Cloud masking is a process used to eliminate cloud bias in the results of the AFP and PFP hotspot classifications (Suwarsono et al., n.d.). Cloud objects are identified based on visible, near infrared and thermal infrared bands as in formula 3:

$$\text{CLD} = \rho_{0.65} + \rho_{0.86} > 0.7 \text{ and } T_{12.4} < 285 \text{ K} \quad (2-3)$$

### c. Water masking

Water and land objects are extracted using the normalised difference vegetation index (NDWI) algorithm (Suwarsono et al., n.d.). This index uses NIR and SWIR bands which show water content at canopy level (Haikal, 2014) and can be used to identify dry and wet areas. It can distinguish water and land objects based on formula 4:

$$\text{WTR} = \frac{\rho_{0.51} - \rho_{0.86}}{\rho_{0.51} + \rho_{0.86}} \quad (2-4)$$

### d. Sunglint masking

The sunglint effect causes bias in the classification of hotspots because it appears as high temperatures and so confuses the extraction. Based on Suwarsono et al., (n.d.), results with solar zenith angle (SoZ) of more than 30% are not classified as hotspots.

### e. Determination of firespots

In this study, firespots are the locations of forest/land fires that actually occur. There are three categories of firespot, drawn from the Landsat 8 images, the field survey data and the burnout data. Determination of firespots from composite Landsat 8 654 images

uses pixels with orange or yellowish-red colour. Also, these fire pixels are associated with smoke. The firespot is visually plotted in the centre of the fire pixel. Firespots from field survey and burnout data are determined based on GPS plotting of the coordinates of fire locations.

#### f. Buffering at 2 km from firespots

Firespot buffering with a radius of 2 km give the possibility of misleading hotspots of 2 km buffer being identified. This distance was chosen with consideration of the spatial resolution of Himawari-8, to allow for estimation that in a 2 km buffer there will be a forest/land fire.

#### g. Validation

Hotspot validation is the process of calculating the accuracy of extracted hotspots against the actual location of forest/land fires. Parameters considered in this validation include:

1. Time of firespot being appropriate to the recording time of the Landsat 8 image.
2. Time of firespot being appropriate to the time of the fire being extinguished.
3. Time of firespot being appropriate to the time of field survey.
4. Hotspots matching with firespots hourly at 09.00 and 10.00 West Indonesia Time (WIB) are then identified as hourly hotspots.
5. Hotspots matching with day of firespot in the time range between 08.00 and 14.00 WIB are identified as daily hotspots.

Zubaidah et al. (2014) devised a formula for an accepted hotspot validation test which in this study was adjusted for Himawari-8 hotspot validation by using the same criteria for

valid hotspots, the number of missing or error hotspots and the total number of hotspots as in formula 5:

$$\text{Accuracy} = (V) / (H + E) \times 100\% \quad (2-5)$$

where V = valid hotspot; H = total number of Himawari-8 hotspots in a selected location; E = number of hotspots missing (there is a fire but no hotspot is detected).

Omission and commission errors are calculated according to formulas 6 and 7:

$$\text{Error commission} = (H - V) / (H + E) \times 100\% \quad (2-6)$$

$$\text{Error omission} = (E) / (H + E) \times 100\% \quad (2-7)$$

## 3 RESULTS AND DISCUSSION

### 3.1. Location and time of firespots

The first category of firespot is matched with the Landsat 8 recording on 28 September 2019 at 02.34 UTC (09.34 WIB). The hotspots in Central Kalimantan are located in four zoning areas as shown in Figure 3.1. The points of fire on 28 September 2019 at 09.34 were in Pulang Pisau Regency, Kapuas Regency, Hulu Sungai Selatan Regency, Tapin Regency and Palangkaraya City. In the images, we can be sure that the location is on fire as indicated by the presence of fire and smoke pixels.

Burnout location is the land on which forest/land fires occur. Recording of burnout coordinates is carried out at the position of the fire. The burnout data are for Kapuas Regency and are sourced from the local BPBD. Table 3.1 explains the burnout data.



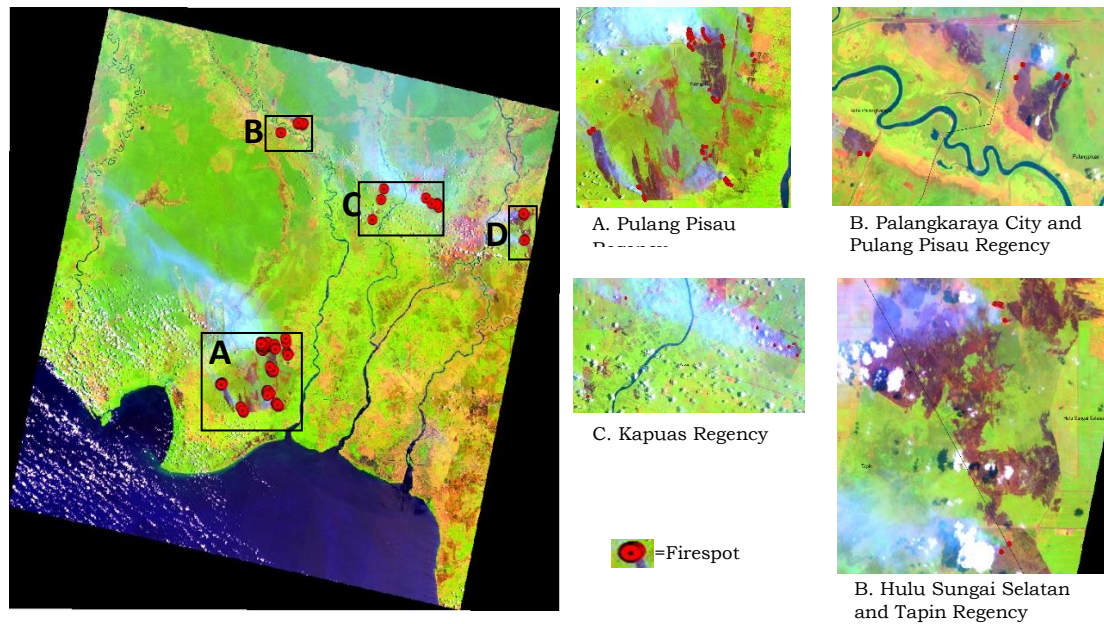


Figure 3.1. Location of firespots from Landsat 8 on 28 September 2019 at 09.34 WIB

Table 3.1 Burnout Data for Kapuas Regency

No	Date	Village	Sub-district	Lon	Lat	Estimated burned area (ha)
1	3 Sept	Palingkau Jaya Sp1	Kapuas Murung	114.50989	-2.81870	1.5
2	8 Sept	Mantangai Hulu	Mantangai	114.52200	-2.47280	50
3	9-11 Sept	Bina Sejahtera A7	Kapuas Murung	114.72389	-2.69917	30
4	21 Sept	Basuta Raya	Kapuas Barat	114.50889	-2.70500	10
5	25 Sept	Pangkalan Rekan	Basarang	114.32334	-3.03613	5
6	25-26 Sept	Anjir Serapat Barat	Kapuas Timur	114.46725	-3.06955	2.1
7	26 Sept	Mantangai Tengah	Mantangai	114.40800	-2.47970	2
8	26 Sept	Bina Jaya A1	Dadahup	114.63339	-2.66824	10
9	27 Sept	Tajepan	Kapuas Murung	114.54110	-2.80600	3
10	3-4 Oct	Harapan Baru A4	Dadahup	114.63444	-2.79283	24
11	3 Oct	Sido Mulyo	Mantangai	114.56281	-2.52550	10
12	4-5 Oct	Baguntan Raya	Bataguh	114.24500	-3.17707	75
13	5 Oct	Ds. Dadahup	Dadahup	114.57690	-2.65941	3
14	5 Oct	Pulau Kaladan	Mantangai	114.40694	-2.54333	2
15	7 Oct	Pulau Telo Baru	Selat	114.38837	-2.96666	2.2

There were 15 outbreaks of fire in Kapuas district from 3 September to 7 October 2018. Firespots that occurred were categorised as either daily fires (one day) or more than one day (> one day). Fires in the Kapuas Regency land are dominated by those in inaccessible peatlands which burn underground and

are hard to extinguish, a process taking more than one day. The location of the burnout coordinates can be shifted from the location of the fire, due to difficulty of access when recording the data. Therefore, the location of the fire is buffered to 2 km from the point of extinguishing by firefighters, and is

shown in Figure 3.2.



Figure 3.2. Burnout firespot distribution and buffering of 2km in Kapuas Regency 3 Sept – 7 Oct 2018

Meanwhile, the distribution of field survey locations can be seen in Figure 3.3. Surveys were carried out in Palangkaraya City, Pulangpisau Regency, East Kotawaringin and Kapuas, with a total of 47 fire points identified. Determination of firespots in the field surveys was achieved through two criteria. The first criterion for a firespot was determined directly during fire surveys themselves, for example in Pulangpisau District. This point of fire has a fire time in accordance with the time of the field survey of between 10:00 and 16:00 WIB. However, several fires at the time of the survey were already burning at 10.00 so these firespots were estimated to have burned for one day. The second criterion for firespot

determination was based on the location of the burned area with additional information on the time of fire gathered from fire officers at that location, for example in Palangkaraya City. This burning location has a fire time in the daily range because the fire lasted for at least 1 day.



Figure 3.3. Field survey firespot distribution

### 3.2. Location and time of AFP and PFP hotspots

Absolute fire pixel (AFP) and possible fire pixel (PFP) Himawari 8 hotspots were extracted for the Central Kalimantan region from 1 September to 6 October 2018 at 08.00 to 14.00. In that time span, hotspot monitoring was carried out every hour, so that every day there seven hotspot times were recorded for each Central Kalimantan region for the two types of hotspots. For the validation test, the hotspot time is adjusted to the time of the available firespot data.

Table 3.2. Number of AFP and PFP hotspots

Validation category	Hotspot category	Hotspot criteria	Number of hotspots
1 Landsat 8	AFP	hourly	67
	AFP	daily	212
	PFP	hourly	229
	PFP	daily	701
2 Field survey	AFP	daily	257
	PFP	daily	3560
3 Burnout data	AFP	daily	133
	PFP	daily	1302

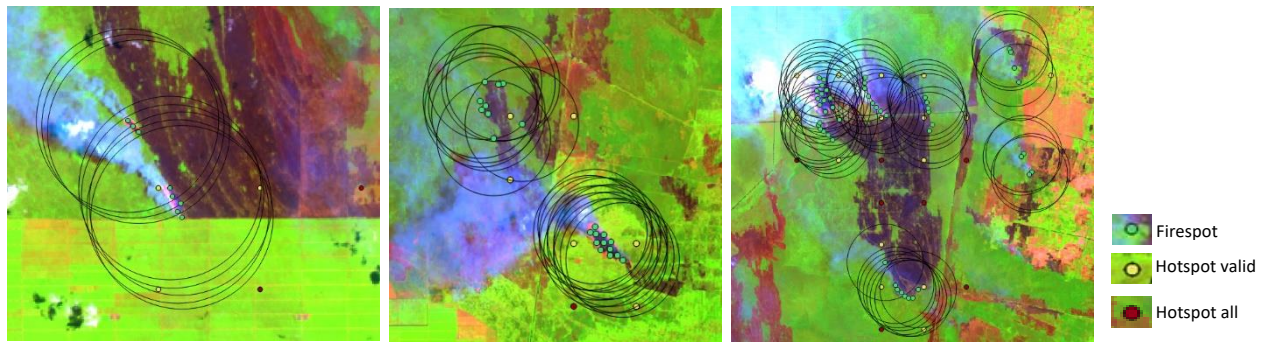


Figure 3.4. Sample of AFP hourly hotspots

Hotspot filters are applied based on time and location according to available hotspot data. There are three validation categories: (1) Landsat 8 images, (2) field survey data and (3) burnout data. In addition there are two hotspot criteria for the validation: (1) hourly hotspots, namely hotspots that have the same recording times of 09.00 and 10:00 and (2) daily hotspots, namely hotspots that have the same recording day period of between 08.00 and 14.00.

The validation test for category 1 is based on Landsat 8 firespots and AFP and PFP hotspots tested on 28 September 2018 between 8:00 and 14:00. In addition, these category 1 hotspots are divided into two categories, hourly and daily. Validation category 2 is based on survey data adjusted to the four district locations at the time the survey was conducted, while validation category 3 is based on burnout data and AFP and PFP hotspots specifically tested in Kapuas district at the time of burnouts meeting daily hotspot criteria. The number of hotspots for each of these criteria can be seen in Table 3.2.

### 3.4. Validation of AFP and PFP hotspots

The validation process determines valid hotspots, missing hotspots, and the total number of hotspots. Valid hotspots as shown in Figure 3.4 are within a radius of 2km from the point of a fire, symbolised by a yellow dot. Missing

hotspots are symbolised by red dots. The total number of hotspots are the yellow and red hotspots combined. The validation test of category 1 based on Landsat 8 imagery can be seen in Figure 3.4. for validation of AFP hourly hotspots.

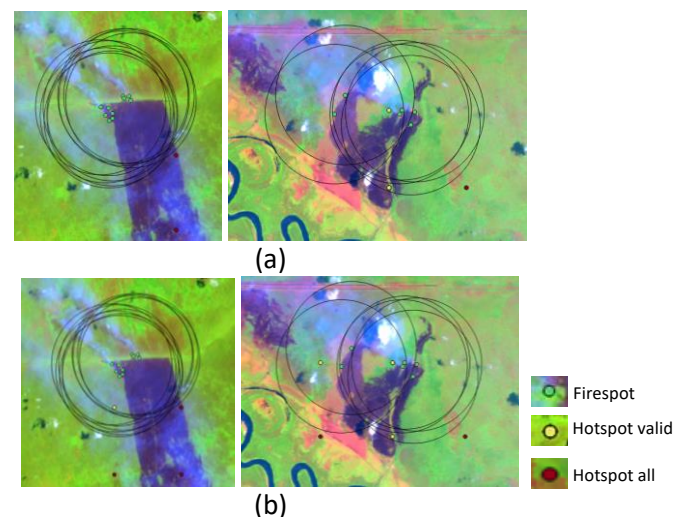


Figure 3.5. Sample of (a) hourly AFP hotspot compared with (b) daily hotspot

Category 2 validation tests based on field surveys are shown in Figure 3.6, which gives an example of an AFP hotspot validation test based on firespots in the field survey data. AFP hotspots can be seen in the picture on the upper-right, and are detected forming a line, indicating that the points represent extension of the fire over a period of time. However, due to limited survey data only two hotspots were declared valid. The entire location of the fire was not reached during the field survey so only fire tip data was obtained.





Figure 3.6. AFP hotspot validation based on field survey data

Meanwhile, the fire spread to the south. This caused the category 2 hotspot validation value to be low. The bottom right picture is an example of a fire location in an urban area but no hotspots were detected. This is because at that location the area of the fire did not reach 4 km<sup>2</sup> (the minimum area of fire detected from the Himawari-8 images).

In urban areas, at a pixel area of 4km<sup>2</sup> corresponding to the pixel resolution of Himawari-8, fires mix with other land cover so that they are detected as mixels with a dominant as build-up land, not as hotspots. It can be said that Himawari-8 hotspots are not good at detecting fires in urban areas because of the influence of other objects in a pixel. Category 3 validation tests

based on burnout data can be seen in Figure 3.7 for PFP hotspots. Valid hotspots are symbolised by yellow dots, while purple dots are PFP recordings in the span of 8 September to 7 October, 2018 that are numerous and lined up representing extensions of fires. However, the limited availability of burnout data, being only at the location of the green dots, makes the number of valid hotspots low. Yellow buffering indicates the firespot is detected as a hotspot while the white buffer is a missing hotspot, indicating there is a fire but no hotspot. The purple dot is a PFP hotspot around the burnout location. It should be kept in mind that hotspot recording is based on imagery, and so all areas are recorded, while burnout data is carried out at certain locations if there are fires reported.



Figure 3.7. Sample of PFP hotspot validation based on burnout data

### 3.5. Validation results

Himawari-8 hourly hotspot AFP data recorded at 09.00 and 10.00 (two readings) validated with Landsat-8 found 67 AFP hotspots. 44 valid hotspots were identified while 29 missing hotspots were identified, representing fire recorded but not detected as hotspots. Accuracy is 45.83% with commission error of 23.95% and omission error of 30.20%. Daily AFP data, which was recorded for 08.00 to 14.00 (seven hours) found 212 hotspots. There were 115 valid hotspots while the number of missing fire detections was 12. The number of missing hotspots here is lower than for the hourly detections, hence accuracy is higher, at 51.33%. The commission error, which represents hotspots identified but no fire being present is higher, at 43.30% but omission error is low, at 5.35% indicating many fires were detected as hotspots.

The Himawari-8 PFP data recorded at 09.00 and 10.00 (hourly readings) found 229 hotspots. However the valid hotspots were only found to be 80, giving lower accuracy of 34%. This is because hotspot location is less accurate as shown from the high commission error rate of 63.67%. For the PFP data over 7 hours, 701 hotspots were found but only 195 were real fires. This represents accuracy of 27.62% with high

commission error rate of 71.67% but with low omission error of 0.70%. This is because given the number of hotspots detected almost all the fires were covered.

This method can be compared with Zubaidah et al. (2014), who validated MODIS hotspots with FIRMS-NASA and Indofire. They achieved accuracy of 64% (CE and OE 18%) for FIRMS-NASA and 42% (CE 38% and OE 20%) for Indofire. In the present study, Himawari-8 AFP hotspot accuracy is between the above values, at 51%, and has higher commission error and lower omission error than the MODIS hotspot findings.

Based on Table 3.3., validation test category 1 drawn from Landsat 8 imagery has the highest accuracy. This is because Landsat 8 imagery records all fires in a certain area at a particular time. AFP daily data has more valid hotspots, so the validation value is higher than for the AFP hourly data. The low accuracy values of categories 2 and 3, which are sourced from survey and burnout data, reflect data limitations meaning they do not cover all locations. This means the total number of hotspots is not proportional to the amount of fire data available. In addition, the burnout and survey data was located at the edge of the fires while the hotspot detected the pixel centre with distance of more than 2 km.

Table 3.3. Accuracy values of Himawari-8 AFP and PFP hotspots

Validation category	HS category	HS criteria	HS number (H)	HS valid (V)	HS missing (E)	Accuracy	CE	OE
Landsat 8	AFP	hourly	67	44	29	45.83	23.95	30.20
	AFP	daily	212	115	12	<b>51.33</b>	43.30	5.35
	PFP	hourly	229	80	5	34.18	63.67	2.13
	PFP	daily	701	195	5	27.62	71.67	0.70
Field survey	AFP	daily	257	15	28	5.26	84.91	9.82
	PFP	daily	3560	424	14	11.86	87.74	0.39
Burnout data	AFP	daily	133	8	13	5.47	85.61	8.90
	PFP	daily	1302	210	3	16.091	83.67	0.22

HS = hotspot; CE = commission error; OE = omission error

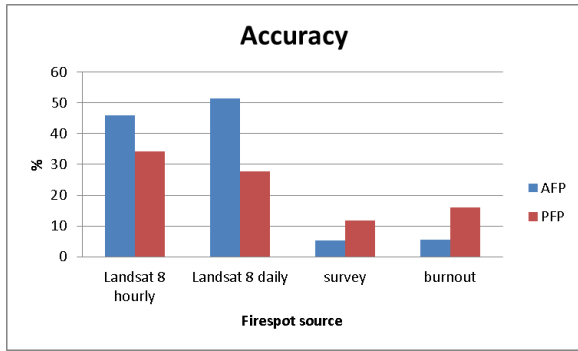


Figure 3.8 Accuracy validation for category 1, 2, and 3 data

A comparison of accuracy values between the categories can be seen in Figure 3.8. The total number of hotspots affects the accuracy value: the greater the number of hotspots, the lower the accuracy value. The number of AFP hotspots detected is less than the PFP hotspots at the Landsat 8 recording location, so that the accuracy of the AFP

hotspots is better than for the PFP hotspots. In addition, the accuracy of the AFP data is better than the PFP hotspot when viewed from field survey data (Figures 3.9 and 3.10). Figure 3.9 is the condition of AFP hotspots in the field. The area is peatland with land cover vegetation dominated by shrubs and interspersed with acacia and oil palms. Fires in the area cause thick smoke and spread over a large area, as can be seen from the distribution of smoke and the number of hotspots detected. In addition, if seen from the mapping of a drone at 100 m, the area is covered by a white layer of smoke from the fire. Meanwhile PFP hotspot field conditions can be in the form of fire or other hot surfaces such as zinc roofs of buildings or sand beds, as shown in Figure 3.10.

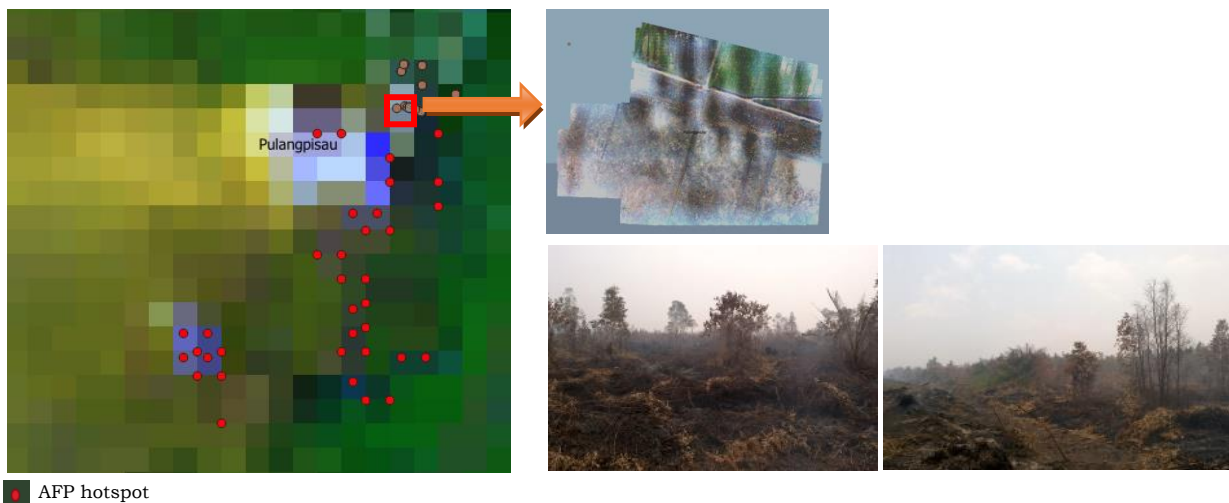


Figure 3.9 Field survey of AFP hotspot

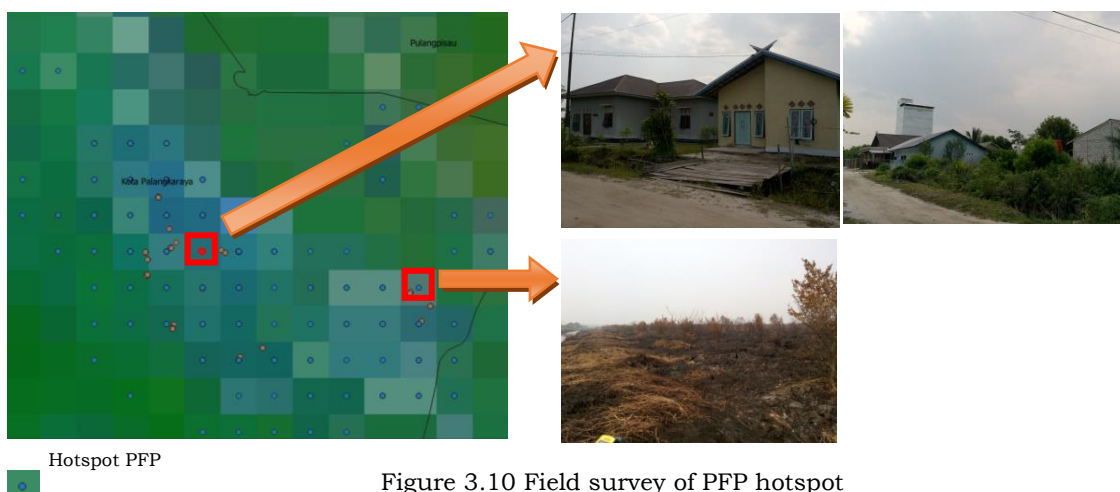


Figure 3.10 Field survey of PFP hotspot

#### 4 CONCLUSION

Validation of Himawari-8 hotspots can be divided into three categories, based on Landsat 8 images, field surveys and burnout data. Of these, validation based on Landsat 8 images has the highest accuracy value. The AFP daily hotspot criteria has the highest accuracy value based on Landsat 8 imagery, of 51.33%. An AFP daily hotspot is a hotspot with the same recording day across a time range of 08.00 to 14.00 WIB. The other categories have lower values due to limited survey and burnout data and so are not proportional to the total number of hotspots record for all regions. The Himawari-8 absolute fire pixel (AFP) hotspots have a higher accuracy value than the possible fire pixel (PFP) hotspots. Field surveys show AFP hotspots in the form of fires on peatlands, while for the PFP hotspots, field surveys show hot surfaces that can be in the form of burning land, zinc roofs of buildings or sand beds.

#### ACKNOWLEDGEMENTS

The field survey in this study was funded by DIPA Remote-Sensing Application Centre LAPAN. The authors would like to thank Dr M. Rokhis Khomarudin as the Head of Remote-Sensing Application Centre LAPAN which has supported this study. This research is the part of SAFE Project LAPAN-JAXA, JAXA, as provider of Himawari-8 data. Also, thanks are due for the support of field survey team members Parwati Sofan, M.Sc. and Gigih Giarrastowo, S.Pi.

#### AUTHOR CONTRIBUTIONS

Hotspot Validation Of Himawari-8 Based On Multisource Data In Central Kalimantan. Lead Author: Khalifah Insan Nur Rahmi; Co-Author: Sayidah Sulma and Indah Prasasti.

#### REFERENCES

- Choi, Y. Y. & Suh, M.-S. (2018). Development of Himawari-8/ Advanced Himawari Imager (AHI) land surface temperature retrieval algorithm. *Remote Sensing*, 10(12). doi:10.3390/rs10122013
- Fitriana, H. L., Sulma, S., Suwarsono, Zubaidah, A., & Prasasti, I. (2018). Spectral analysis of the Himawari-8 data for hotspot detection from land/forest fires in Sumatra. *International Journal of Remote Sensing and Earth Sciences* 15(1), 15–24.
- Giglio, L., Csiszar, I., & Justice, C. O. (2006). Global distribution and seasonality of active fires as observed with the Terra and Aqua Moderate Resolution Imaging Spectroradiometer (MODIS) Sensors. *Journal of Geophysical Research*, 111, 1–12. doi:10.1029/2005JG000142
- Giglio, L., Schroeder, W. & Justice, C.O. (2016). The Collection of 6 MODIS active fire detection algorithm and fire products. *Remote Sensing of Environment* 178, 31–41. doi:10.1016/j.rse.2016.02.054
- Guangmeng, G., & Mei, Z. (2004). Using MODIS land surface temperature to evaluate forest fire risk of Northeast China. *IEEE Geoscience and Remote Sensing Letters* 1(2), 98–100. doi:10.1109/LGRS.2004.826550.
- Haikal, T. (2014). *Analisis Normalised Difference Wetness Index (NDWI) Dengan Menggunakan Data Citra Landsat 5 TM (Studi Kasus: Provinsi Jambi Path/Row: 125/61) [Normalised difference wetness index (NDWI) analysis using Landsat 5 TM image data (Case study: Jambi Province path/row: 125/61)*. Undergraduate Thesis, IPB University.
- Hally, B., Wallace, L., Reinke, K., & Jones, S. (2016). Assessment of the utility of the Advanced Himawari Imager to detect active fire over Australia. *International Archives of the Photogrammetry, Remote Sensing and Spatial Information Sciences*, 41, 65–71. doi:10.5194/isprsarchives-XLI-B8-65-2016



- Hayasaka, H., Noguchi, I., Putra, E. I. Yulianti, N., & Vadrevu, K. (2014). Peat-Fire-Related Air Pollution in Central Kalimantan, Indonesia. *Environmental Pollution*, 195, 257–66. doi:10.1016/j.envpol.2014.06.031
- Zubaidah, A., Vetrina, Y., & Rokhis Khomarudin, M. (2014). Validasi Hotspot MODIS di Wilayah Sumatera dan Kalimantan Berdasarkan Data Penginderaan Jauh SPOT-4 Tahun 2012: 1–15 [Validation of MODIS hotspots in Sumatra and Kalimantan region based on SPOT-4 remote sensing data for 2012: 1–15]. *Jurnal Penginderaan Jauh* 11, 1–14.
- JMA (2017). *Himawari Standard Data User's Guide*. Tokyo: JMA.
- Kushardono, D. (2012). Kajian Satelit Penginderaan Jauh Cuaca Generasi Baru Himawari 8 Dan 9 [The new generation of satellite weather sensing satellite studies Himawari 8 and 9]. *Jurnal Inderaja*, 3(5), 41–49.
- LAPAN (2015). Pedoman Pemanfaatan Data Landsat-8 Untuk Deteksi Daerah Terbakar (Burned Area) [Data utilization guidelines Landsat-8 for detection of fire region (burned area)]. Jakarta: Pusat Pemanfaatan Penginderaan Jauh LAPAN.
- LAPAN (2016). Informasi Titik Panas (Hotspot) Kebakaran Hutan/Lahan [Information on forest/land fire hotspots]. In Parwati, A. Widipaminto, Suwarsono, A. Zubaidah, A. Indrajat, & N. D. Salyasari (Eds.) (1st ed). Jakarta: Deputi Bidang Penginderaan Jauh LAPAN.
- Noor, M. (2019). Kebakaran Lahan Gambut [Peatland fire]. Yogyakarta: UGM Press.
- Osaki, M., Nursyamsi, D., Noor, M., Wahyunto, & Segah, H. (2016). Peatland in Indonesia. In M. Osaki & N. Tsuji (Eds.), *Tropical Peatland Ecosystems* (pp. 49–58). Tokyo: Springer. doi:10.1007/978-4-431-55681-7\_3
- Pandjaitan, B. S. & Panjaitan, A. (2015). Pemanfaatan Data Satelit Cuaca Generasi Baru Himawari 8 Untuk Mendeteksi Asap Akibat Kebakaran Hutan Dan Lahan Di Wilayah Indonesia (Studi Kasus: Kebakaran Hutan Dan Lahan Di Pulau Sumatera Dan Kalimantan Pada Bulan September 2015) [Utilization of new generation Himawari 8 weather satellite data to detect smoke due to forest and land fires in Indonesian territory (Case Study: forest and land fires on Sumatra and Kalimantan Island in September 2015)] *Seminar Nasional Penginderaan Jauh 2015*: 636–51. doi:10.13140/RG.2.2.27568.05120
- Puspa, A., Sukaesih, I. and Syaufina, L. (2016). Hotspot pattern distribution in peat land area in Sumatera based on spatio-temporal clustering. *Procedia Environmental Science* 33, 635–45. doi: 10.1016/j.proenv.2016.03.118
- Suwarsono, Sulma, S., Fitriana, H. L. Zubaidah, A. Prasasti, I. & Rokhis Khomarudin, M. (Submitted for publication). Fire Hotspot Detection Using Advance Himawari Imager Sensor in Sumatera and Kalimantan Using Multithreshold Technique. *TELKOMNIKA (Telecommunication Computing Electronics and Control)* 13(2), 1–8.
- Tanpipat, V., Kiyoshi, H., & Prayoonyong, N. (2009). MODIS hotspot validation over Thailand. *Remote Sensing* 1(4), 1043–1054. doi:10.3390/rs1041043
- USGS (2019). *Landsat 8 (L8) Data Users Handbook Version 5.0*. South Dakota: USGS.
- Vlassova, L., Pérez-Cabello, F., Mimbbrero, M. R., Montorio Lloveria, R. & Garcia-Martin, A. (2014). Analysis of the relationship between land surface temperature and wildfire severity in a series of Landsat Images, *Remote Sensing* 6, 6136–62. doi:10.3390/rs6076136

